Supporting Information to

CCl_3^+ and CBr_3^+ Salts with the $[Al(OR^F)_4]^-$ and $[(^FRO)_3Al\text{-}F\text{-}Al(OR^F)_3]^-$ Anions

Anna Lehner, Nils Trapp, Harald Scherer and Ingo Krossing*

* Albert-Ludwigs-Universität Freiburg, Institut für Anorganische und Analytische Chemie and Freiburger Materialforschungszentrum FMF, Albertstr. 21, D-79104 Freiburg i. Br., Germany, phone: +49 761 203 6122, e-mail: krossing@uni-freiburg.de

Contents

1. NMR Spectrocopy

In situ reactions were done in sealed NMR tubes that were filled from a three valve reactions vessel shown in the following figure on the right:

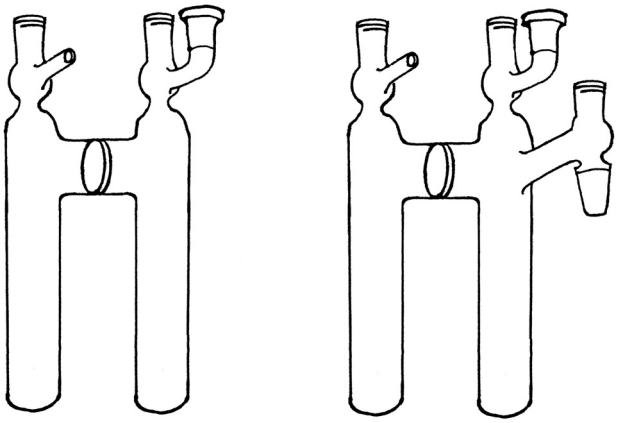

All other reactions were done in the two valve vessel shown left.

Further NMR Spectra of the CX_3^+-salts:

Stability and visibility of CCl_3[pftb]: Temperature effects.

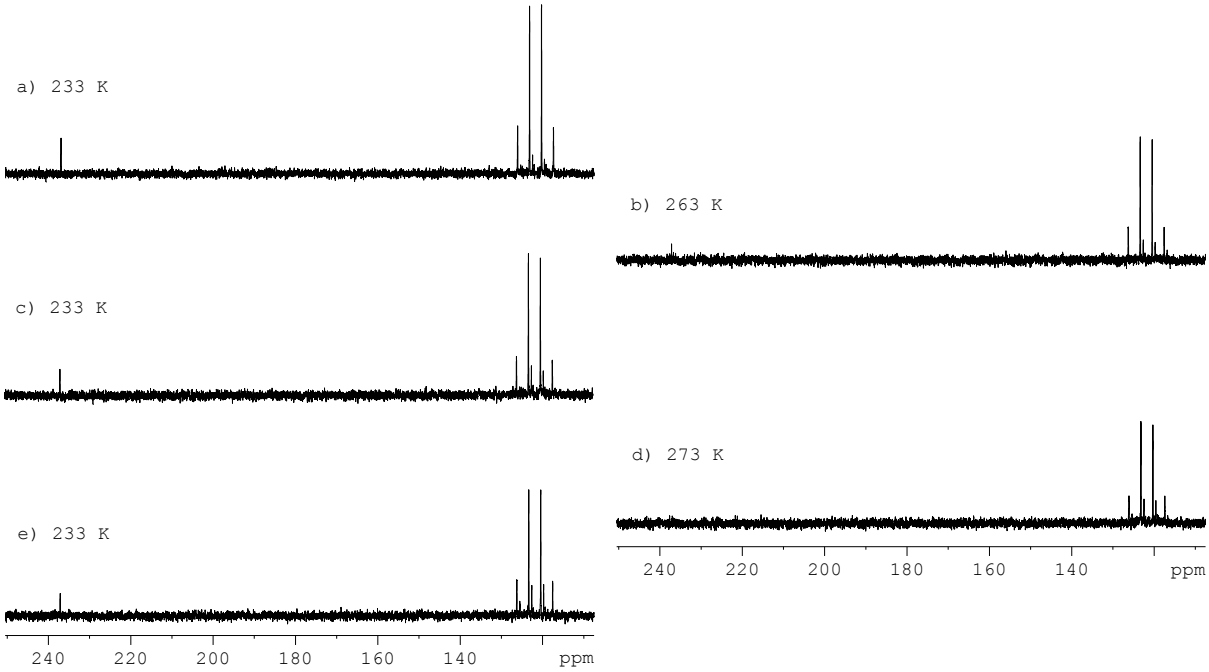

^{13}C-NMR-Spectra of CCl_3[pftb] in SO_2ClF (100,6 MHz). a) at the day of the filtration, NS = 860, –40 °C, b) 10 days later, NS = 512, –10 °C, c) same day, lower temperature NS = 512, –40 °C, d) after 15 days; NS = 512, 0 °C, e) same day, lower temperature, NS = 512, –40 °C.

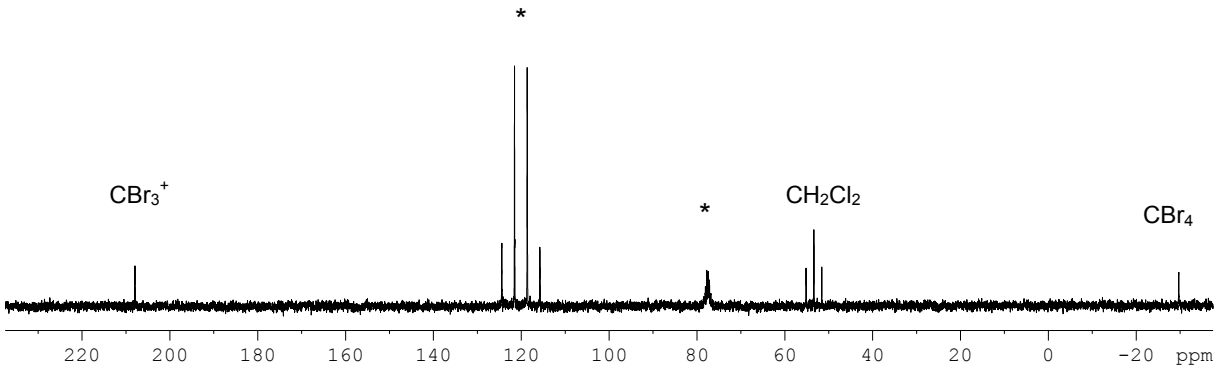

^{13}C-NMR-Spectrum of CBr_3[al-f-al] in SO_2 at –30 °C: Excess CBr_4 from the reaction is visible; CH_2Cl_2 stems from the $Ag(CH_2Cl_2)_x$[al-f-al] used (x ≈ 1-2).

Decomposition of the Anion in CBr_3[al-f-al]: Temperature effects.

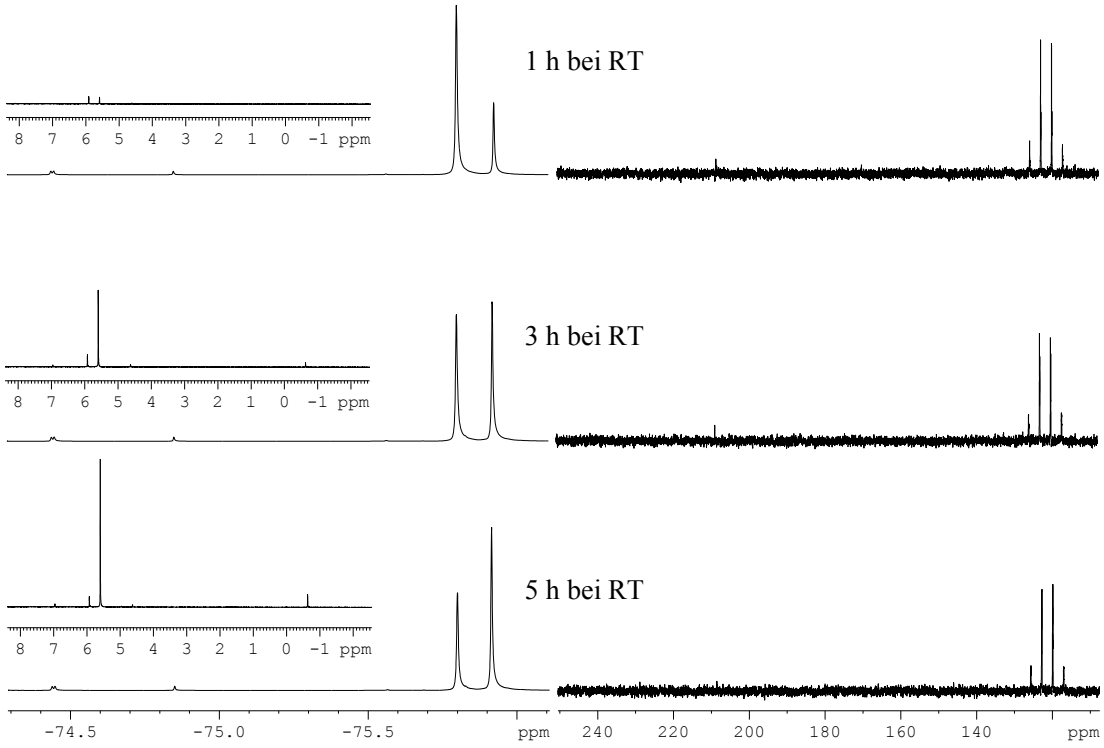

Sections of the ^{19}F-(376,5 MHz) and ^{13}C-(100,6 MHz)-NMR-Spectra of CBr_3[al-f-al] in SO_2 at RT (left: ^{19}F-NMR-Spectra, right: ^{13}C-NMR-Spectra, upper trace: 1 h at RT, middle: 3 h at RT, lower trace: 5 h at RT).

2. Vibrational Spectroscopy of 1 to 4

S-Table 1: Experimental and calculated IR-data of $CBr_3[Al(pftb)_4]$ (3) und $CCl_3[Al(pftb)_4]$ (1).

exp. IR **(1)** [a] / [cm^{-1}]	exp. IR **(3)** [a] / [cm^{-1}]	calc. IR-Bands $[Al(pftb)_4]^-$ [b] / [cm^{-1}]	calc. IR-Bands Banden CBr_3^+ [b] / [cm^{-1}]	calc. IR-Bands Banden CCl_3^+ [b] / [cm^{-1}]	Assignment
-	519 (m)	520 (vw)			F-C-F
-	537 (m)	547 (w)			F-C-F, O-Al-O
-	561/571 (w)				
728 (s)	727 (s)	711 (m)			Al-O, F-C-F
743 (w)	743 (w)	738 (w)			Al-O, F-C-F
833 (w)	832 (w)	823 (w)			Al-O
877 (m)			**860 (w)**		**CBr_3^+, e'**
975 (s)	973 (s)	961 (m)			C-C, C-F
975 (s)	-	1110 (w)			C-C, C-F
	1038 (m)			**1011 (w)**	**CCl_3^+, e'**
1178 (m)	1179 (m)	1141 (w)			C-C, C-F
1218 (s)	1219 (s)	1216 (s)			C-C-C, C-C, C-F
1249 (s)	1248 (s)	1232 (s)			C-C-C, C-F
1264 (s)	1265 (s)	1263 (s)			C-C, C-F
1300 (m)	1299 (m)	-			-
1354 (s)	1353 (w)	1338 (m)			C-O, C-C

[a] ZnSe-ATR (ATR-corr.), [b] b-p/SV(P)

S-Table 2: Experimental and calculated IR-data of CBr_3[al-f-al] (4) and CCl_3[al-f-al] (2).

Exp. IR **(2)** [a] / [cm^{-1}]	exp. IR **(4)** [a] / [cm^{-1}]	calc. IR-Bands [al-f-al]$^-$ [b] / [cm^{-1}]	calc. IR-Bands CBr_3^+[b] / [cm^{-1}]	calc. IR-Bands CCl_3^+[b] / [cm^{-1}]	Assignment
538 (m)	538 (m)	520 (w)			F-C-F, Al-F-Al
573 (m)	572 (m)	560 (w)			F-C-F, Al-O
643 (m)	639 (m)	635 (w)			Al-F-Al
728 (s)	728 (s)	710 (m)			F-C-F, Al-O
-	-	790 (vw)			Al-O, C-C-F
841 (w)	837 (w)	846 (vw)			Al-O, Al-F-Al
-	865 (w)	856 (vw)			Al-O, Al-F-Al
877 (m)			**860 (w)**		**CBr_3^+, e'**
975 (s)	975 (s)	965 (m)			O-C-C, C-F
	1038 (m)			**1011 (w)**	**CCl_3^+, e'**
-	-	1111 (vw)			C-C, C-F
1187 (m)	1183 (m)	1145 (vw)			C-C, C-F
1218 (s)	1218 (s)	1211 (m)			C-C, C-F, C-C-C
1250 (s)	1249 (s)	1236 (s)			C-C, C-F
1268 (m)	1268 (m)	1263 (m)			C-F, C-C
1301 (m)	1301 (m)	-			-
-	-	1332 (m)			C-O, C-C, C-F
1356 (w)	1355 (w)	1347 (w)			C-O, C-C

[a] ZnSe-ATR (ATR-korr.), [b] BP86/SV(P)

Infrared spectra of all compounds overlaid with experimental spectra of the starting silver salts and IR simulations at the BP86/SV(P) level of isolated CX_3^+, isolated $[A]^-$ as well as an overlay of the latter

two giving the simulated $[CX_3]^+[A]^-$ spectrum.

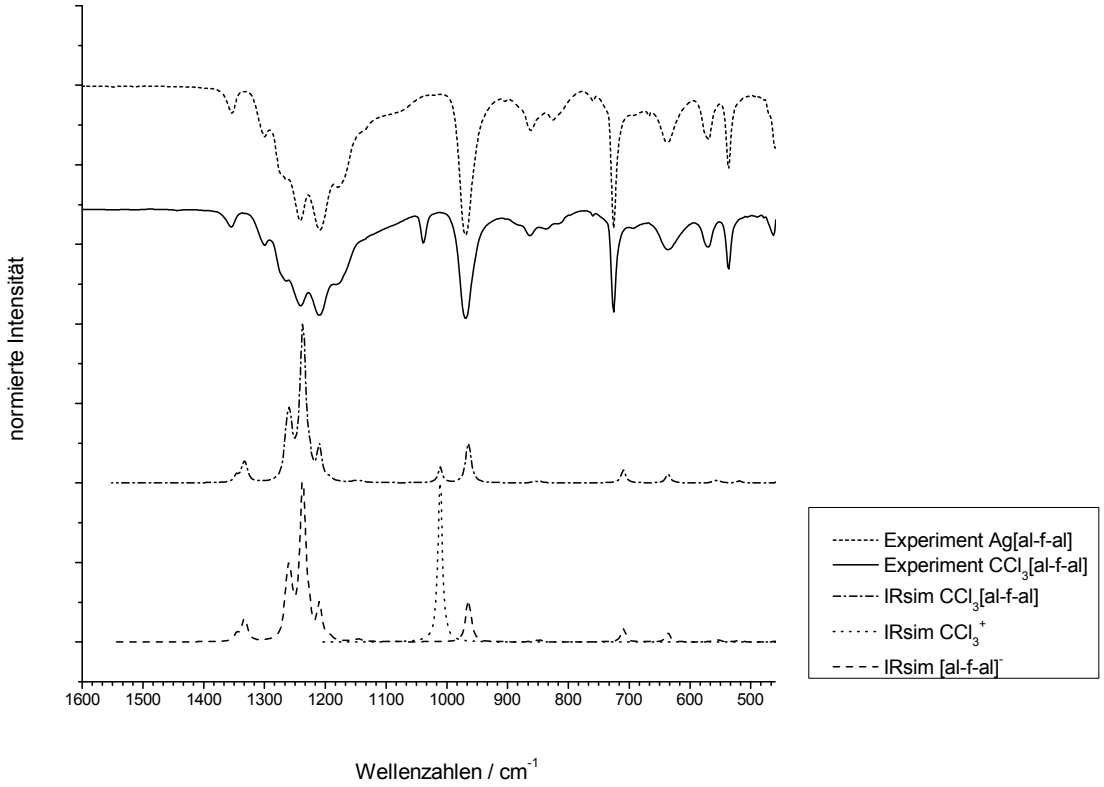

S-Figure 1: Simulated and experimental ATR-IR-Spectra of CCl_3[al-f-al] (2).

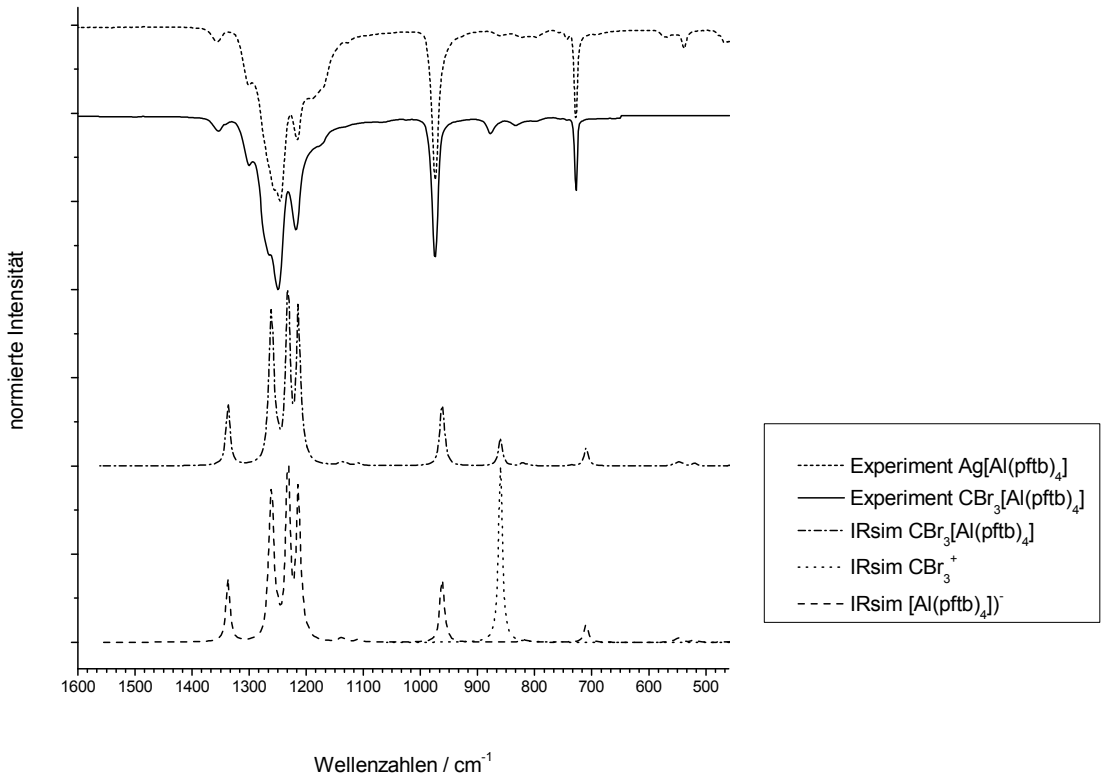

S-Figure 2: Simulated and experimental ATR-IR-Spectra of $CBr_3[Al(pftb)_4]$ (3).

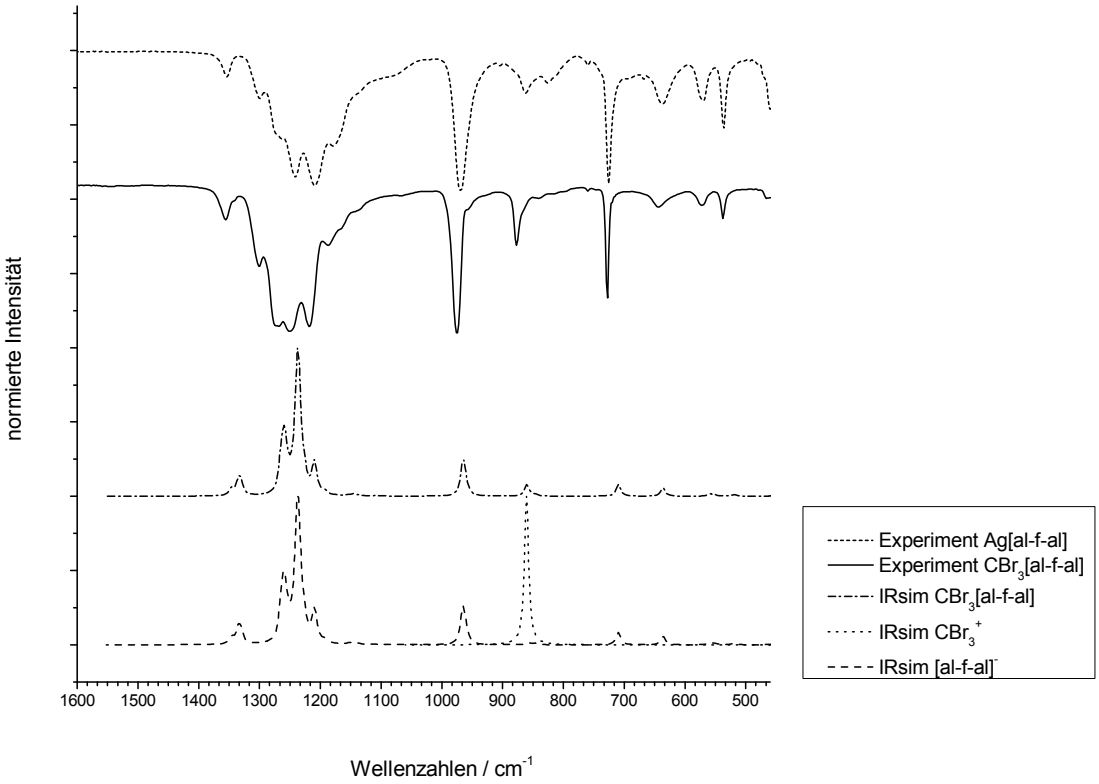

S-Figure 3: Simulated and experimental ATR-IR-Spectra of CBr_3[al-f-al] (4).

3. Details of the partial crystal structure of **1**

Kristallographische Daten zur Kristallstruktur von $CCl_3[Al(OC(CF_3)_3)_4]$ (**1**).

Kristallgröße [mm]	0.2 x 0.3 x 0.2
Kristallsystem	orthorhomisch
Raumgruppe	$Pna2_1$
Dimensionen der Elementarzelle	a = 17,2(3) Å, α = 90°
	b = 10,6(2) Å, β = 90°
	c = 17,9(4) Å, γ = 90°
V [Å ^{3}]	3256.2(11)
Z	4
ρ_{ber} [kg m^{-3}]	2214,2
μ [mm^{-1}]	0,546
Absortpionskorrektur	numerisch
F (000)	2088
Bereich der Indices	$-20 \le h \le 20$, $-11 \le k \le 12$, $-21 \le l \le 20$
Messbereich θ	3,05 bis 24,71
Temperatur [K]	193
Diffraktometer Typ	Rigaku Spider
unabhängige Reflexe [$I > 2\sigma(I)$]	7303
Datenpunkte / Beschränkung / Parameter	5543 / 146 / 671
GOOF	2,606
finaler R1 [$I > 2\sigma(I)$]	0,1281
finaler wR2	0,3583
Größter Rest-Reflex [e Å^{-3}]	0,929
Größtes Rest-Loch [e Å^{-3}]	0,670

Tabelle 3: Atomkoordinaten (x 10^4) und äquivalente isotrope Auslenkungsparameter (Å^2 x 10^3) für (3).

U(eq) ist definiert als 1/3 der Spur des orthogonalisierten U_{ij} Tensors.

	x	y	z	U(eq)
C	148(3)	111(5)	2470(5)	384(17)
Cl(1)	–397(3)	–1121(5)	2414(4)	169(2)
Cl(2)	962(2)	98(6)	2910(3)	109(2)
Cl(3)	–94(4)	1443(4)	2100(4)	131(2)
CA	–106(3)	–65(5)	2225(6)	114(7)
Cl(1A)	228(5)	–1317(7)	2648(3)	224(5)
Cl(2A)	–943(3)	–79(6)	1805(3)	113(2)
Cl(3A)	410(3)	1214(5)	2146(4)	125(2)
Al(1)	–2547(1)	–661(1)	4852(1)	30(1)
O(1)	–2496(2)	–2259(3)	4863(5)	86(2)
O(2)	–3031(3)	–221(6)	5608(3)	82(2)
O(3)	–3009(3)	–123(5)	4059(2)	65(1)
O(4)	–1625(2)	–54(3)	4844(3)	57(1)
C(5)	–3458(3)	–107(4)	6200(3)	63(2)
C(6)	–4276(3)	–586(4)	6028(3)	166(7)
F(10)	–4672(4)	342(7)	5674(4)	292(8)
F(11)	–4217(3)	–1657(5)	5599(3)	110(2)
F(12)	–4633(4)	–905(8)	6691(4)	308(6)
C(7)	–3287(3)	–800(4)	6946(3)	132(5)
F(13)	–2553(3)	–556(7)	7073(4)	243(3)
F(14)	–3740(4)	–323(8)	7476(3)	255(5)
F(15)	–3414(4)	–2012(6)	6822(4)	241(4)
C(8)	–3567(3)	1255(5)	6453(3)	195(5)
F(16)	–3612(3)	2049(5)	5885(4)	235(5)
F(17)	–2950(4)	1582(7)	6861(3)	261(5)
F(18)	–4184(3)	1423(9)	6881(4)	431(5)
C(6A)	–4166(5)	–839(5)	5873(3)	41(6)
F(10A)	–4524(5)	6(7)	5314(4)	22(3)
F(11A)	–4336(13)	–2029(7)	5476(6)	500(80)
F(12A)	–4839(5)	–889(9)	6380(5)	27(3)
C(9)	–3483(2)	–95(3)	3442(3)	60(2)
C(10)	–4315(3)	–685(4)	3538(3)	131(6)
F(19)	–4261(4)	–1670(6)	3935(4)	189(4)
F(20)	–4679(5)	214(8)	3847(5)	431(14)
F(21)	–4542(5)	–907(8)	2872(4)	313(4)

C(11)	–2936(3)	–910(4)	2928(3)	230(5)
F(22)	–2990(4)	–697(7)	2203(3)	232(4)
F(23)	–2178(3)	–920(7)	3047(3)	137(2)
F(24)	–3143(5)	–2117(5)	2999(3)	162(3)
C(12)	–3501(3)	1346(5)	3238(3)	325(7)
F(25)	–3627(4)	1966(9)	3875(4)	273(6)
F(26)	–4112(4)	1401(8)	2778(4)	385(5)
F(27)	–2849(4)	1689(8)	2903(3)	254(4)
C(10A)	–3940(3)	–1366(6)	3401(3)	27(7)
F(19A)	–4144(6)	–1899(12)	4040(5)	52(7)
F(20A)	–3374(7)	–1900(18)	3016(7)	410(110)
F(21A)	–4482(8)	–760(20)	3021(8)	1100(500)
C(13)	–1082(2)	858(4)	4895(2)	60(2)
C(14)	–1178(2)	1850(5)	4250(3)	154(4)
C(15)	–260(3)	230(4)	4852(2)	103(3)
C(16)	–1157(2)	1562(4)	5675(3)	162(4)
F(28)	–912(4)	1422(8)	3629(3)	304(4)
F(29)	–809(3)	2862(5)	4432(5)	187(4)
F(30)	–1896(2)	2167(5)	4153(3)	117(2)
F(31)	–159(4)	–419(5)	5472(3)	156(2)
F(32)	282(2)	1100(5)	4810(4)	146(2)
F(33)	–172(3)	–545(4)	4288(3)	99(2)
F(34)	–1243(3)	693(6)	6194(3)	177(4)
F(35)	–570(3)	2260(7)	5842(4)	230(4)
F(36)	–1787(4)	2246(5)	5639(4)	149(3)
C(1)	–2189(2)	–3427(4)	4848(2)	43(1)
C(2)	–1484(3)	–3454(4)	4282(2)	167(6)
F(1)	–1665(5)	–2556(6)	3708(3)	197(5)
F(2)	–853(3)	–3067(6)	4752(5)	150(4)
F(3)	–1424(4)	–4726(6)	4011(4)	160(3)
C(3)	–2827(3)	–4409(5)	4595(3)	300(20)
F(4)	–2630(3)	–5539(4)	4773(4)	124(3)
F(5)	–3478(3)	–4128(5)	4898(4)	122(3)
F(6)	–2883(6)	–4312(10)	3877(3)	258(7)
C(4)	–1899(3)	–3734(5)	5666(3)	372(12)
F(7)	–1580(4)	–2734(6)	5934(3)	144(3)
F(8)	–2493(4)	–4058(7)	6053(4)	175(5)
F(9)	–1398(4)	–4636(6)	5642(5)	162(3)
C(2A)	–1894(3)	–4006(5)	4144(3)	54(6)

F(1A)	–1426(5)	–3089(7)	3685(5)	46(3)
F(2A)	–2110(9)	–4891(9)	3515(6)	2000(800)
F(3A)	–1216(5)	–4772(9)	4438(6)	57(4)
C(3A)	–2772(4)	–4322(5)	5137(3)	86(10)
F(4A)	–2693(12)	–5615(8)	5002(5)	430(50)
F(5A)	–3271(8)	–3795(13)	4604(6)	230(20)
F(6A)	–3071(9)	–4126(12)	5852(5)	86(5)
C(4A)	–1527(3)	–3476(5)	5375(4)	41(5)
F(7A)	–2022(5)	–2866(8)	5835(8)	183(15)
F(8A)	–906(5)	–2752(9)	5208(8)	80(5)
F(9A)	–1313(8)	–4604(10)	5657(12)	350(40)

Unit cell representation showing the packing of **1** and omitting all $C(CF_3)_3$ groups as well as the disordered sites.

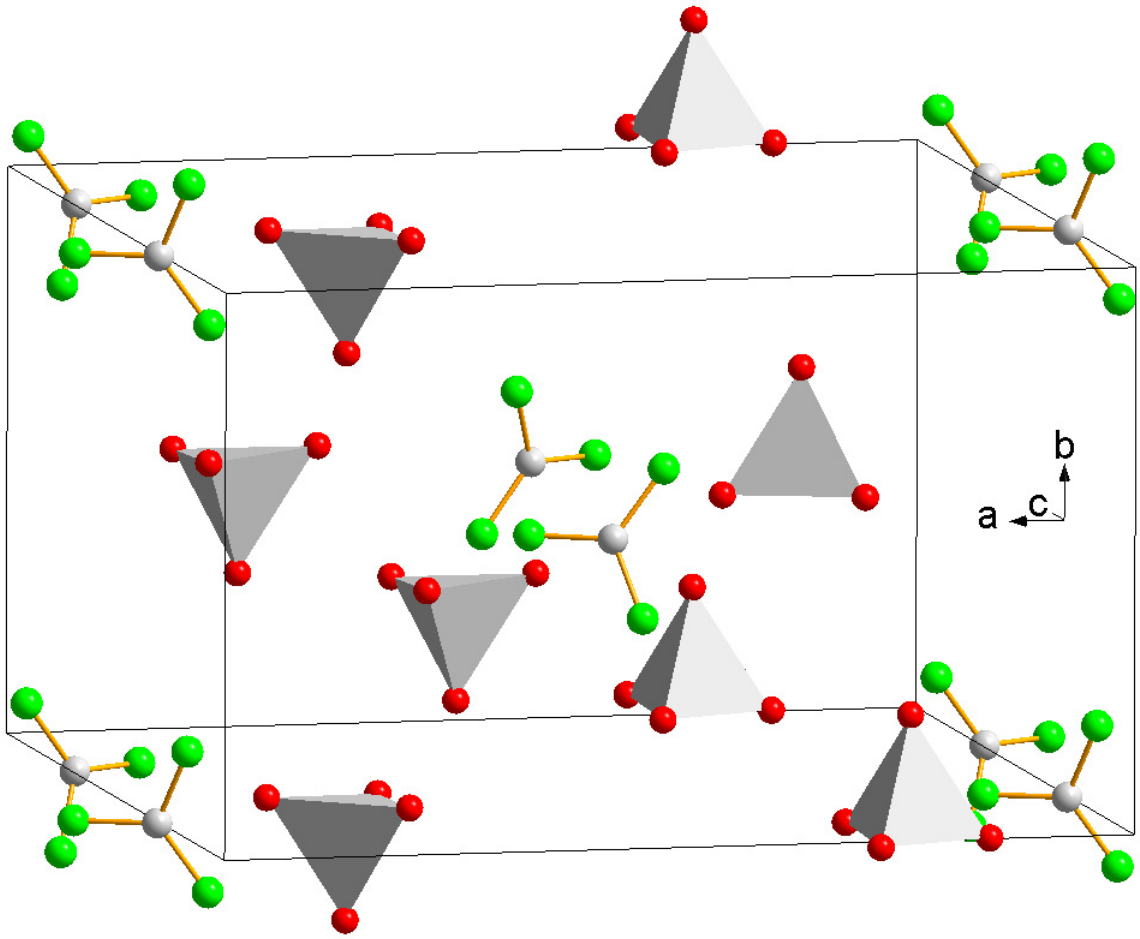

4. UV-Vis Spectra

To assign the UV-Vis Spectra the MO-Diagram of CX_3^+ was calculated at the BP86/SV(P) level and the UV-Vis spectra were calculated by TD-DFT/BP86/SV(P):

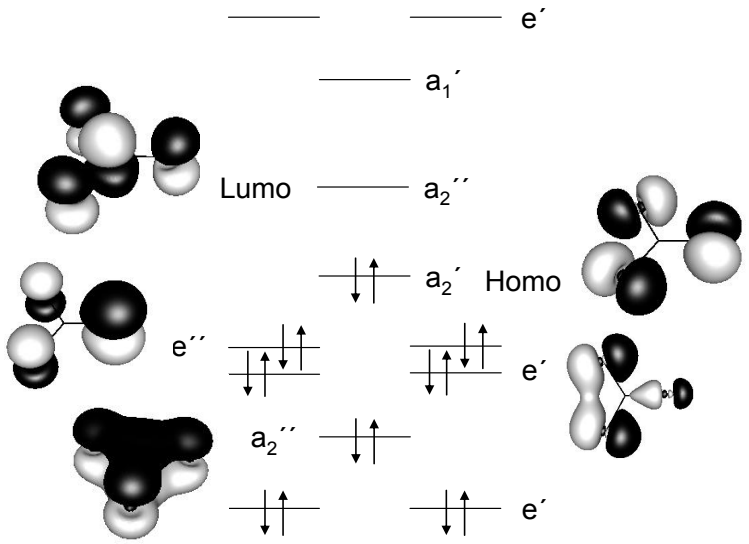

Calculated [a] UV/Vis-Bands at lowest energy for CX_3^+ and BX_3 (X= Cl, Br, I), experimental values in parentheses.

Bande /nm	CI_3^+	CBr_3^+	CCl_3^+	BI_3	BBr_3	BCl_3
a	231 (274)[b]	176	137	198	143	115
b	309 (307)[b]	214	159	233	167	133
c	384 (349)[b]	291	231	293 (313)[c]	224 (206)[d]	183 (172)[d]

[a] TD-DFT at b-p/SV(P), [b] from Ref. [45], [c] from Ref. [85], [d] from Ref. [86].

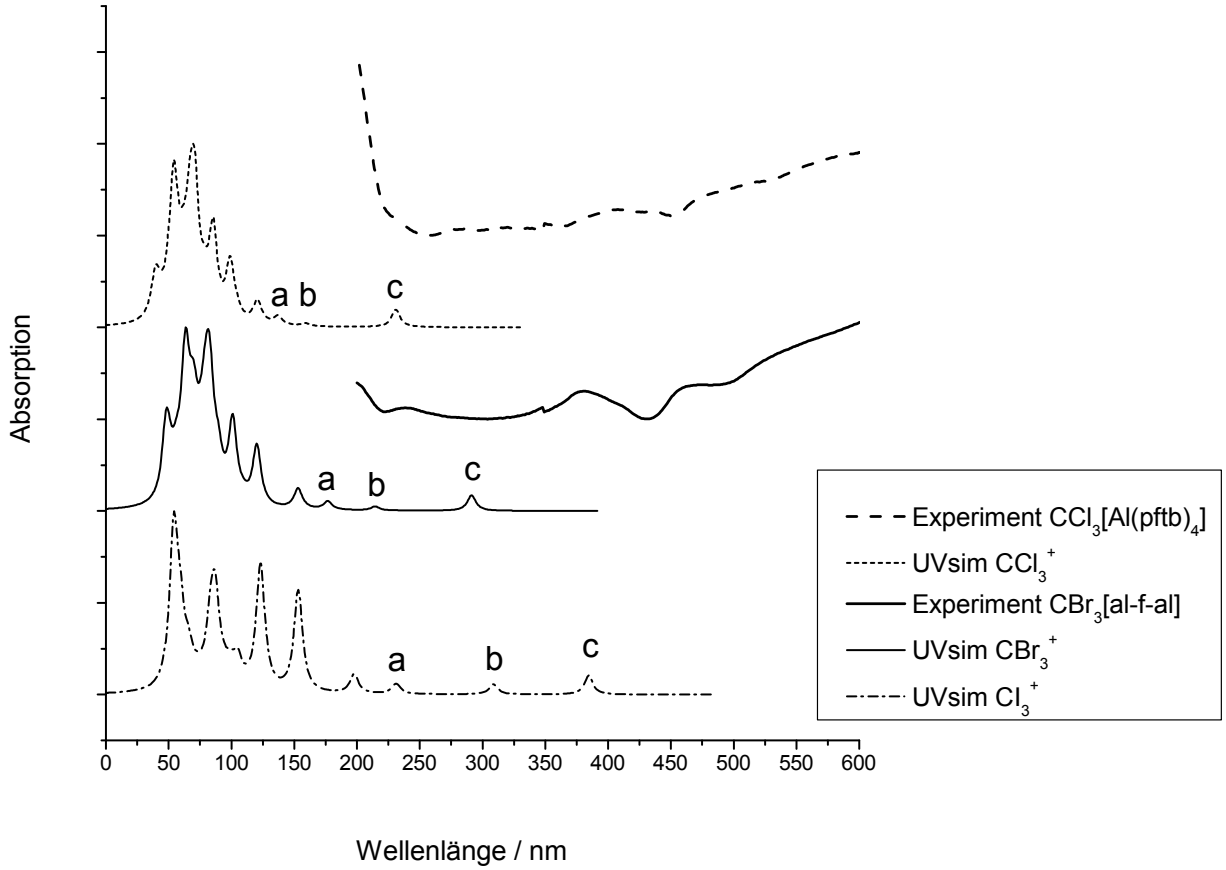

Experimental UV/Vis-Spectra of (**1**) and (**4**), calculated (b-p86/SV(P)) spectra of the CX_3^+-cations. The small hard edge at 350 nm is attributed to the automatic change of the lamps.

5. Quantum chemical calculations

Calculated energies (DFT-pbe0 and MP2) for the reactions $CCl_3^+ + SO_2 \rightarrow SO_2\text{-}CCl_3^+$ and $SO_2ClF\text{-}CCl_3^+ + SO_2 \rightarrow SO_2ClF + SO_2\text{-}CCl_3^+$:

Molecule	Method / basis set	Symmetry	U (0 K) [kJ/mol]	H (273 K) [kJ/mol]	G (273 K)[a] [kJ/mol]	G_{solv} (SO_2ClF, 273 K)[a] [kJ/mol]]	ZPE[a] [kJ/mol]
CCl_3^+	pbe0/def2-TZVPP	D_3h	-3722716,5	-3722682,0	-3722765,2	-3722835,1	22,44
SO_2	pbe0/def2-TZVPP	C_2v	-1439853,7	-1439825,5	-1439898,6	-1439896,7	18,39
SO_2ClF	pbe0/def2-TZVPP	C_s	-2909768,0	-2909716,9	-2909807,7	-2909803,9	36,19
$SO_2\text{-}CCl_3^+$	pbe0/def2-TZVPP	C_1	-5162604,7	-5162537,8	-5162667,7	-5162731,8	42,62
$SO_2ClF\text{-}CCl_3^+$	pbe0/def2-TZVPP	C_1	-6632516,7	-6632428,3	-6632574,7	-6632636,7	60,01
CCl_3^+	MP2/def2-TZVPP	D_3h	-3719741,4	-3719706,9	-3719790,1	-3719860,0	22,44
SO_2	MP2/def2-TZVPP	C_2v	-1438663,2	-1438635,0	-1438708,1	-1438706,1	18,39
SO_2ClF	MP2/def2-TZVPP	C_s	-2907448,7	-2907397,6	-2907488,4	-2907484,6	36,19
$SO_2\text{-}CCl_3^+$	MP2/def2-TZVPP	C_1	-5158447,8	-5158380,9	-5158510,8	-5158574,9	42,62
$SO_2ClF\text{-}CCl_3^+$	MP2/def2-TZVPP	C_1	-6627233,0	-6627144,5	-6627290,9	-6627352,9	60,01

[a] Thermodynamic corrections based on pbe0/def2-TZVPP calculations (scaling factor: 0.97).

Cartesian MP2/def2-TZVPP minimum geometries of all calculated compounds:

CCl_3^+:

0.00000000000000	0.00000000000000	0.00000000000000	c
1.55054201525109	-2.68561754968513	0.00000000000000	cl
1.55054201525109	2.68561754968513	0.00000000000000	cl
-3.10108403050219	0.00000000000000	0.00000000000000	cl

SO_2:

0.00000000000000	0.00000000000000	-0.91888645907061	s
-2.36595548460867	0.00000000000000	0.45944322953530	o
2.36595548460867	0.00000000000000	0.45944322953530	o

SO_2ClF:

-0.00000101043026	0.11778210567373	0.38011017526731	s
-2.36511469870708	0.20671099244038	1.62749784249890	o
2.36510983693370	0.20671260657701	1.62750325848896	o
0.00000160859211	2.26379106992375	-1.62546095025312	f
0.00000426361152	-2.79499677461488	-2.00965032600207	cl

SO_2-CCl_3^+:

-0.89774898012440	2.65848409084441	0.01213488168651	c
1.48480768680809	3.95317120942842	1.51322327912202	cl
-3.59736467779822	2.23672264479068	1.47501583917103	cl
-0.60022241621298	1.84404100467930	-2.96167903601570	cl
1.46847295512593	-4.36289461335804	0.43524681350015	s
1.44412158990354	-4.22017406322224	-2.29682240113980	o
0.69793384229807	-2.10935027316243	1.82288062367576	o

SO_2ClF-CCl_3^+:

-2.46052245535481	3.04963343972875	-1.46721983404705	c
-0.29482447426454	4.63731651199350	-3.01452660704475	cl
-3.43065330350026	4.05596106977011	1.29935128149783	cl
-3.69590725737754	0.49440007063355	-2.70903859862743	cl
1.68349772605222	-2.33818373709006	1.03642171214235	s
0.07892505069130	-3.96349306602907	-0.36249674256716	o
1.38302727999467	0.34280771943466	0.92772844658651	o
5.24202157170150	-3.19786081152316	0.44426800741452	cl
1.49443586205749	-3.08058119691832	3.84551233464512	f